

Medium PRF Radar PRF Selection Using Evolutionary Algorithms

C M Alabaster, E J Hughes and J H Matthew

Abstract—Previous work has demonstrated that evolutionary algorithms are an effective tool for the selection of optimal pulse repetition frequency (PRF) sets to minimise range-Doppler blindness in a highly simplified model of a medium PRF radar. In this paper we extend the work considerably by considering the detailed effects of side-lobe clutter and the many technical factors affecting the choice of radar PRF in a medium PRF mode of operation of a practical fire control radar.

The abilities of the evolutionary algorithm are exploited further by not only considering the traditional use of eight PRFs, but also the use of nine, whilst maintaining the ability to transmit all the PRFs within the dwell time on the target. By using 9 PRFs, it is shown that superior blind zone performance can be achieved. Unlike all previous work, the algorithm presented also ensures that all the solutions produced are fully decodable, i.e. can resolve the range and Doppler ambiguities inherent in a medium PRF, and have no blind velocities. It was found that the evolutionary algorithm was able to identify near-optimum PRF sets for a realistic radar system with only a modest computational effort.

Keywords—Medium PRF Radar, Pulsed-Doppler Radar, Evolutionary Algorithms.

I. INTRODUCTION

MANY modern radar systems use medium pulse repetition frequency (PRF) waveforms to measure both target range and velocity accurately in the presence of clutter. Medium PRF radars possess excellent clutter rejection characteristics which render them an attractive proposition for airborne intercept (AI), fire control systems, ground based air surveillance, weapon locating radar and a variety of other applications.

A radar using a single medium PRF generates highly ambiguous range and Doppler data and suffers from a number of blind regions in range and velocity. The ambiguities may be resolved by operating on several PRFs, typically eight, and requiring target data in a minimum number, typically three, in what is known as a three from eight scheme. The problem becomes one of selecting suitable combinations of PRFs to resolve the ambiguities, minimise the blind zones, avoid blind velocities and reduce problems of ghosting, whereby incomplete resolution of the ambiguities in the presence of noise can lead to false targets.

The spread of PRFs is governed by sound engineering principles, based on clutter rejection and target illumination times. However, the traditional approach to the selection of precise values often results in mediocre radar performance. Previous work by the authors [1] has shown that it is possible to use evolutionary algorithms to automate the process of generating near-optimal PRF sets that minimise the blind zones for a simplified radar model. The work did not address the problems of decodability or totally blind velocities. This paper proposes a scheme to automate the selection of precise PRF values to optimise all the aspects of radar performance discussed previously.

Mr Clive M. Alabaster and Dr Evan J. Hughes are with the Department of Aerospace, Power and Sensors, Cranfield University, Royal Military College of Science, Shrivenham, Swindon, England, SN6 8LA. Tel. +44 (0)1793 785255, Fax. +44 (0)1793 785902, ejhughes@ieee.org

Existing techniques to resolve the ambiguities are based on the Chinese remainder theorem and the coincidence or unfolding algorithm. An excellent review of medium PRF radar and PRF selection is provided by Long and Harringer [2]. Conventionally, the Chinese remainder theorem has employed pulse repetition intervals ($PRI = 1/PRF$) of integer numbers of range cells and subsequent modulo mathematics which is sufficiently simple to enable a hardware solution [3]. However, integer mathematics imposes limitations on the number of suitable PRFs and does not address the minimisation of blind zones. The coincidence algorithm is more computationally intensive for small numbers of targets but removes certain constraints on the PRF selection (section II-C). This paper proposes a scheme based on the coincidence algorithm and utilises a near continuous range of PRFs which creates a vast search space which, in turn, compounds the problem of PRF selection but enables superior solutions to exist. Since an exhaustive search of PRF combinations is not possible, evolutionary algorithms have been employed. PRF set selection is made on the basis of resolving ambiguities, removing blind velocities and minimising blind zones in the range/velocity space.

Section two describes the factors influencing the choice of PRF sets for a medium PRF radar and of the proposed timing rationale. Section three presents a radar model based on an airborne fire control type radar. The crucial issues of clutter modelling and its influence on the blind zone map are discussed. Section four describes the evolutionary algorithm and how it is applied to the problem. Finally, the fifth section discusses the results in which the performance of 8 and 9-PRF schedules are considered and performance statistics generated from Monte-Carlo trials. The paper concludes that an evolutionary algorithm is a powerful technique for optimising the selection of PRFs and ensuring that a medium PRF radar can not only resolve range and velocity ambiguities but maximise its detection performance in all aspects. The results show that a 3 of 9 system has better blind zone performance than a 3 of 8 system and by using the evolutionary approach, solutions can be found that can still be transmitted within the dwell time on the target.

II. MEDIUM PRF RADAR

A. Introduction

The main advantage of low-PRF radar is the ability to measure target range directly using simple pulse delay ranging. However, low-PRF radar suffers from a lack of Doppler visibility, since mainbeam clutter and undesired slow moving targets occupy most of the spectrum. As a result, an excessive number of target returns are rejected along with mainbeam clutter. Furthermore, low-PRF waveforms suffer from severe Doppler ambiguities. Low-PRF radar is best suited to operation in the

absence of ground clutter returns. The principle advantage of high-PRF radar, is the ability to detect high closing-rate targets, whose Doppler frequencies fall clear of sidelobe clutter, in what is essentially a noise-limited environment. However, detection performance is poor in tail aspect (low closing-rate) engagements, where targets compete directly with the Doppler spectrum of the sidelobe clutter. Furthermore, the highly ambiguous range response causes the sidelobe clutter to fold within the ambiguous range interval. Consequently, sidelobe clutter can only be discarded by resolving in Doppler frequency. Medium-PRF radar is a compromise solution designed to overcome some of the limitations of both low and high-PRF radar. By operating above the low-PRF region, the ambiguous repetitions of the mainbeam clutter spectrum may be sufficiently separated without incurring unreasonable range ambiguities. Consequently, the radar is better able to reject mainbeam clutter through Doppler filtering without rejecting too many targets. By operating below the high-PRF region, the radar's ability to contend with sidelobe clutter in tail-chase engagements is improved. Targets may now be extracted from sidelobe clutter using a combination of Doppler filtering and range gating.

B. PRF Selection

Each PRF is characterised by regions of blind velocities and ranges associated with the Doppler filtering of mainbeam clutter and time gating of sidelobe clutter and associated eclipsing losses. These blind zones are depicted in black on a blind zone map, as in figures 1 & 2.

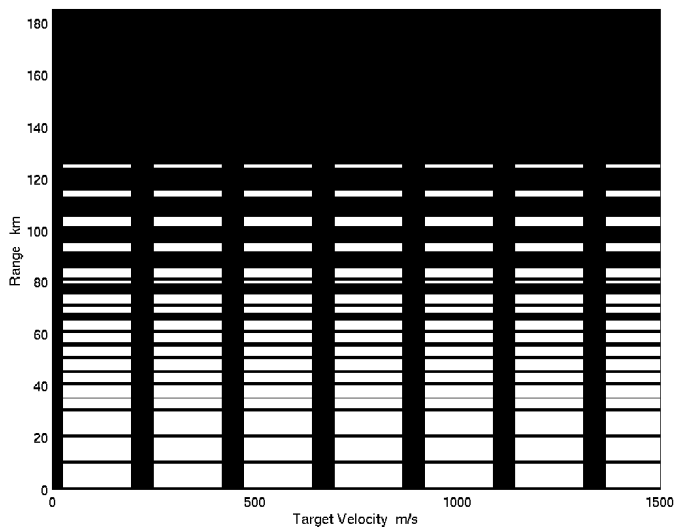


Fig. 1. Blind zones for a single, clutter limited, medium PRF waveform with PRI $67.26\mu s$

Multiple bursts of pulses are required in order to perform target detection and to resolve range and Doppler ambiguities. This is achieved by transmitting a number of PRFs within the dwell time on target and sequentially measuring and comparing the ambiguous information received from every PRF. All the eight PRFs from a 3 of 8 system must be able to be transmitted within the dwell time, with each PRF burst having 64 pulses (64-point FFT) and a short period of time in which to change over PRFs.

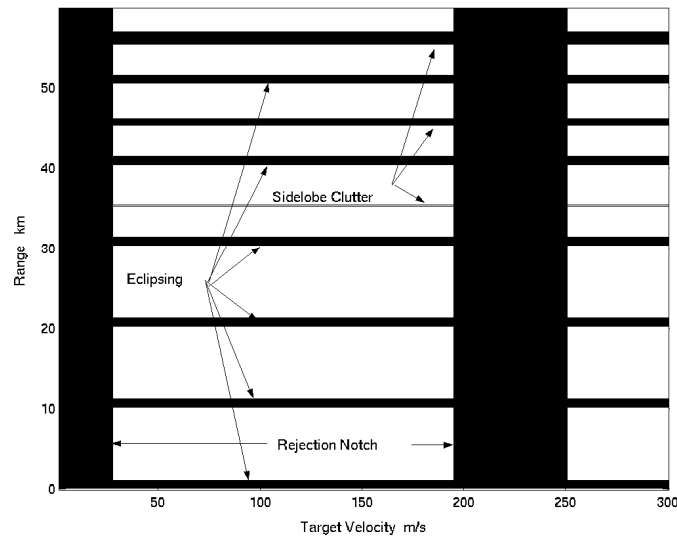


Fig. 2. Expanded view of Blind zones of Fig. 1

The positions of blind zones vary with PRF, therefore, by applying suitable PRFs in a multiple-PRF detection scheme, not only may range and Doppler ambiguities be resolved, but also the blind zones may be staggered to improve target visibility. Ground clutter returns received through the antenna sidelobes may be strong enough to overwhelm weak target signals, consequently blind ranges tend to worsen with increasing range, as shown in figure 3. Figure 4 illustrates its effect on a blind zone map of a 3 from 8 PRF schedule.

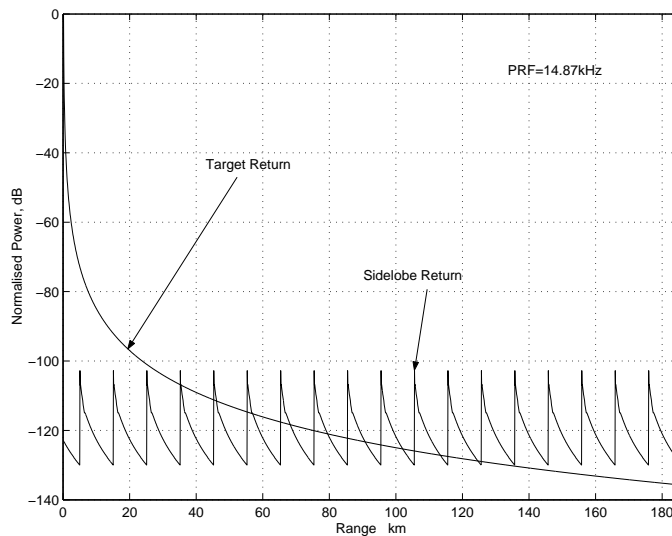


Fig. 3. Comparison of target return and sidelobe clutter for a single, noise limited, medium PRF waveform with PRI $67.26\mu s$

Conventionally, three PRFs are required to be clear in range and Doppler in order to resolve range and Doppler ambiguities and to declare a target detection. However, Simpson [3] shows that, against scintillating targets, the probability of detection is improved substantially if the number of clear PRFs is increased to four. In the blind zone map of figure 4, the black shading represents zones where fewer than three PRFs are clear and, hence,

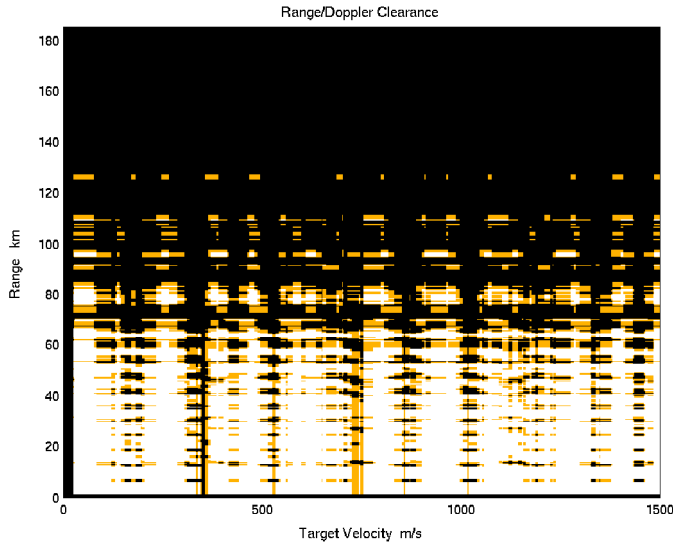


Fig. 4. Blind Zone Map of Target Returns for 8-PRF Schedule ($2m^2$ target)

where the radar is totally blind. The grey shading represents the near-blind zones where three PRFs only are clear. White regions represent zones where four or more PRFs are clear. Figure 4 also indicates blind zones at low velocities (black vertical strip on left) and ranges (black horizontal strip at bottom of figure) which are present in all PRFs due to the clutter rejection, but their repetition, which was evident in figure 1, is now avoided.

The number of PRFs within a schedule must be selected carefully; too few and the ability to overcome range-Doppler blind zones will be hindered. With too many PRFs, then, depending on the average PRF, there may be insufficient time to transmit the entire PRF schedule within the dwell time on target. Typically, eight PRFs are employed spanning about an octave.

If a constant peak power and pulse width is employed, then the average transmitted power and duty cycle will vary proportionally. In an 8-PRF schedule, the total dwell time on target is divided into eight coherent processing intervals. If the number of pulses processed during each interval remains constant, as is usual when FFT Doppler processing is employed, then the processing times will vary, but the probability of detection on each segment will not be affected. Furthermore, as an FFT synthesises a fixed number of contiguous digital filters, the Doppler resolution will vary proportionally with PRF. FFT Doppler processing with a variable duty cycle is the norm and is the method assumed in this paper.

Because of the relatively wide bandwidths of the rejection notches, the possibility remains for a PRF schedule to be decodable and still have some rejection notch overlap; this is found to be a particular problem at the first repetitions of the ambiguous Doppler intervals. The consequences of such occurrences are bands of Doppler frequencies in which the radar is blind, or nearly blind (three PRFs clear only), at *all* ranges, thereby allowing a target to approach at a particular velocity with minimum risk of detection. This is illustrated in figure 4 which shows blindness at all ranges at a velocity of 352m/s. Nothing can be done about the rejection notches, centred on zero Hz, which blind the radar to crossing targets. However, a test for more

than four (3 from 8) or five (3 from 9) rejection notches overlapping outside this region can ensure against PRF schedules being completely range-blind at other target velocities.

The selection of PRFs in a medium PRF set is therefore based on the following:

1. A spread of values which enable the resolution of range and velocity ambiguities,
2. the minimisation of blind zones,
3. removal of totally blind velocities,
4. ensuring that the duty cycle yields the desired average transmitted power,
5. constraints imposed by the practical issues of system timings, e.g. transmitter duty cycle giving an upper bound on the allowable PRF, and average PRI being constrained by the target illumination time [4].

The finer the timing resolution of the PRIs, the greater the number of PRIs within the search space. This in turn increases the complexity of finding an optimum PRF set but also improves the performance of that optimum solution.

Since the minimisation of blind zones is influenced by the size of the target that is anticipated with respect to the levels of sidelobe clutter rejection required, it is imperative to have a reliable model or data on the nature of the clutter. The exact clutter characteristics are likely to be scenario specific and so one must either operate using a PRF set appropriate to averaged conditions or optimise the PRF set dynamically. Section III-B describes the clutter model used in this work.

C. System Timings and Decodability

Simpson [3] describes a scheme by which each PRI is comprised of an integer number of range cells of fixed width. The requirement for the PRI to be an integer multiple of the range cell width stems from the Chinese remainder theorem [5, Sec 17.4] which is applied conventionally for ambiguity resolution. The use of the Chinese remainder theorem highly constrains the PRF selection problem and restricts PRF selection by such a degree that little account of the minimisation of blind zones is possible. In the work by Simpson, the radar model was constrained further, leading to a reduced search space, and only allowed poor solutions to be identified [1].

The radar model of the present study assumes that pulses will be an integer number of cycles of the fundamental system clock and that the range is sampled according to the fundamental clock rate, the ideal continuous search space is not realisable.

To ensure decodability, the Lowest Common Multiple (LCM) of any set of three PRIs from the set of eight (56 possible combinations) must be greater than the time delay of the maximum range of interest. Similarly the LCM of any combination of 3 PRFs must be less than the total Doppler bandwidth.

Additionally, with the Chinese remainder algorithm, all the 56 combinations of three PRIs/PRFs in the set of eight must be co-prime, i.e. the lowest common multiple of each set of three PRIs/PRFs must equal the product of the three PRIs/PRFs, constraining the set of valid PRI schedules dramatically. These extra constraints are not a requirement of the coincidence algorithm [2] and so the coincidence algorithm is assumed in this paper. The coincidence algorithm operates by taking the target returns in a PRI and repeating them until the maximum range

has been covered. For a single PRI, this will give many ranges at which a target may be present. The process is repeated for all the visible PRIs and the results overlaid. If a true target is present, it will appear in the same position in all visible PRIs (yet may not be detected). Likewise, the true Doppler may be resolved in the frequency domain. When accounting for range and Doppler the process can be performed with a two-dimensional map in range-Doppler space.

The decodability test above is satisfactory for an infinitely short pulse. In practice this is not the case. A better check for decodability is to allow for the width of the pulse, and also an allowance for the range extent of the target. This helps to avoid *ghosting* where two PRIs may align partly with a noise detection occurring correspondingly in a third PRI, giving the appearance of a true target. A simple process where extended pulses are placed in arrays at repetitions of the PRI for each PRI and a coincidence check performed will determine practical decodability easily. In this paper, a compressed pulse length of $0.5\mu\text{s}$ is extended to $0.7\mu\text{s}$ for the decodability check. The extra $0.2\mu\text{s}$ allows for the pulse extension resulting from a 30 metre target and therefore reduces the chances of ghosting. If the extra time added to the pulse is increased, it becomes harder to identify fully decodable PRI schedules, and therefore very clear blind zone maps, but does improve the resistance to the formation of ghosts.

III. THE RADAR MODEL

A. Introduction

A radar model based on an airborne fire control type application was derived to trial the fitness of PRF sets. The model assumes 10GHz operation, 64-point FFT processing, linear FM pulse compression achieving a compression ratio of 14 and that platform motion compensation is applied. The maximum target velocity with respect to the ground was taken as 1500 m/s and the maximum range was taken to be 185 km (100 nmi). These and other operational characteristics are summarised in Table I. It is intended that the model should be representative of the types currently in service or about to enter service. Clutter was modelled and resulted in a requirement to reject mainbeam clutter and ground moving targets over a band $\pm 1.67\text{kHz}$. Simulations were performed against a 5m^2 target and result in considerable blindness at long ranges due to overwhelming sidelobe clutter. Larger targets are less easily swamped by sidelobe clutter and detection is maintained at greater ranges.

B. Clutter Modelling

Figure 5 shows a typical range-Doppler clutter map for an airborne fire control radar scenario. The code used to calculate the clutter response is based on the code provided in [6].

Due to the shallow depression angle of the antenna (6° down), the strong mainlobe clutter return is seen at all ambiguous ranges. If platform motion compensation had been incorporated into the clutter map then the mainbeam clutter would be centred on Doppler filter bin zero. The characteristic sawtooth profile of the sidelobe return is evident throughout the Doppler interval. The strong altitude line is also very clear. The clutter map for each PRI will be different as each PRI contains a

Parameter	Value
Carrier frequency	10 GHz
Minimum PRI	$35\mu\text{s}$
Maximum PRI	$150\mu\text{s}$
Transmitted pulsewidth	$7\mu\text{s}$
Compressed pulsewidth	$0.5\mu\text{s}$
Compression technique	Linear FM 2 MHz chirp bandwidth
FFT size	64 bins
Range resolution	75m
Blind range due to eclipsing	15 range cells
Duty cycle	Variable (0.2 peak)
Antenna 3dB beamwidth	3.9°
Antenna scan rate	$60^\circ/\text{s}$
Maximum GMT velocity rejected	25 m/s
Mainlobe clutter/GMT rejection notch bandwidth	$\pm 1.67\text{kHz}$
Maximum target Doppler	$\pm 100\text{kHz}$ (1500 m/s)
Maximum detection range	185.2 km (100 nmi)
Clutter backscatter coefficient	-20 dB
Target radar cross-section	5m^2

different number of range bins.

The sidelobe clutter profiles used in the calculations are based on only the range profiles of the appropriate clutter maps for the PRIs used. The Doppler bins are averaged for each map after notching out the mainbeam clutter return to give a good one dimensional approximation of the full clutter map.

IV. EVOLUTIONARY ALGORITHMS AND THEIR APPLICATION TO THE PROBLEM

A. Introduction

Evolutionary Algorithms are optimisation procedures which operate over a number of cycles (generations) and are designed to mimic the natural selection process through evolution and survival of the fittest [7], [8]. A *population* of M independent individuals is maintained by the algorithm, each individual representing a potential solution to the problem. Each individual has one *chromosome*. This is the genetic description of the solution and may be broken into n sections called *genes*. Each gene represents a single parameter in the problem, therefore a problem that has eight unknowns for example, would require a chromosome with eight genes to describe it.

The three simple operations found in nature, natural selection, mating and mutation are used to generate new chromosomes and therefore new potential solutions. In this paper, new chromosomes were generated by a combination of mating (otherwise

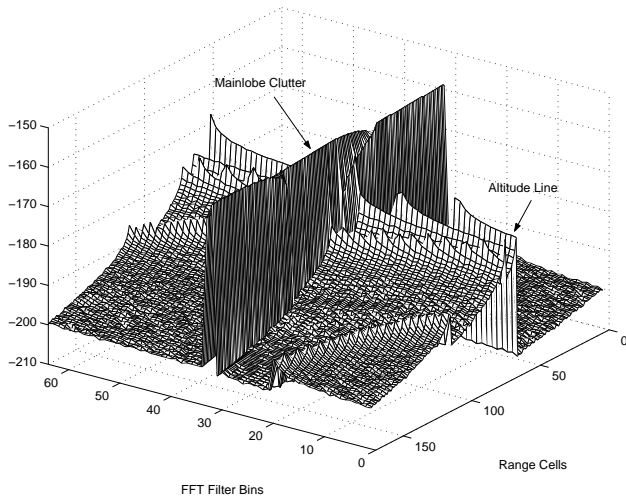


Fig. 5. Range-Doppler clutter map for typical medium PRF ($90.1\mu\text{s}$)

known as *crossover*) and applying Gaussian noise, with a standard deviation that reduced with each generation, to each gene in each chromosome. Each chromosome is evaluated at every generation using an *objective function* that is able to distinguish good solutions from bad ones and to score their performance. With each new generation, some of the old individuals die to make room for the new, improved offspring. Despite being very simple to code, requiring no directional or derivative information from the objective function and being capable of handling large numbers of parameters simultaneously, evolutionary algorithms can achieve excellent results.

A flowchart representing the whole process is given in figure 6. The radar model accepts a chromosome from the evolutionary algorithm and decodes it into a set of PRIs. Operational parameters are passed to the clutter model, which in turn returns clutter data. A blind zone map is created and target visibility is determined. The raw visibility data is then passed back to the evolutionary algorithm as the objective value to drive the evolutionary process. A new generation of PRFs is then produced and the process repeated.

B. Applying evolution to the problem

Earlier work by Davies and Hughes [1] compared evolutionary algorithms and exhaustive search techniques to select medium PRF schedules to minimise blind zones. They concluded that evolutionary algorithms offered an efficient alternative to conventional search methods and that they were capable of finding the optimum, or near optimum, solutions in a fraction of the time taken by the exhaustive search method. The study also suggested that the speed and flexibility of evolutionary algorithm techniques offered the potential for a radar to select PRF schedules optimally from a vast set of possible solutions, in near real-time. The blind-zone maps in this paper cover a range-Doppler space that is over six times larger than the space considered by Davies and Hughes and has a vastly improved clutter model and fifty times as many PRIs to choose from, when using equivalent radar models (11501 compared to

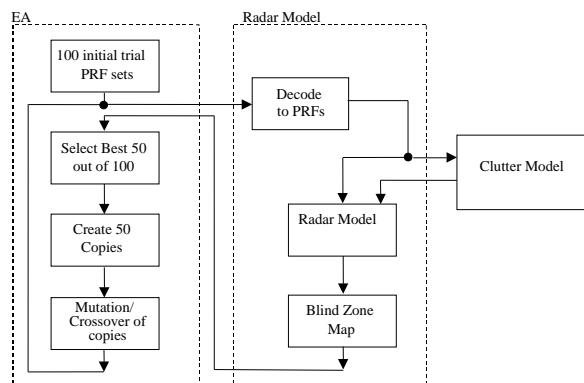


Fig. 6. Flowchart of optimisation process

230).

C. Evolutionary coding strategies

In the present study we optimise the selection of PRIs using a real-value evolutionary algorithm to generate near continuous PRIs and the coincidence algorithm to resolve ambiguities. This scheme ensures that a vast number of PRIs are available to the optimisation process and that the timings of each PRI may be derived from a 100MHz clock. With such a vast search space available to the optimisation process, it has been possible to select PRI sets for ambiguity resolution, minimisation of blind zones and the removal of blind velocities.

Each chromosome forms a trial solution to the problem and consists of a set of eight (or nine) genes that lie in the interval $[0, 1)$. These genes are then decoded into a PRI schedule, which is then used within a radar model to assess the schedule's quality and to ensure that the schedule meets certain constraints. The chromosome is transformed into a PRI set by first generating a set, \mathcal{P} , containing all possible choices of PRI (11501 in the example in this paper). The first PRI is chosen as the i^{th} PRI with i given by the total number of available PRIs ($|\mathcal{P}|$) multiplied by the value of the first gene, giving a choice of 1 in 11501. The PRI chosen is removed from the set \mathcal{P} . The second PRI is chosen in a similar way, this time being a choice of 1 of 11500. The remaining set \mathcal{P} is now checked and any PRIs that are not decodable in both range and Doppler with the two PRIs chosen, or which may lead to severe ghosting are removed from the set \mathcal{P} . Any PRIs that would also lead to a blind velocity are also pruned. The third and subsequent PRIs can now be chosen similarly, given the reduced set of \mathcal{P} , and reducing the set accordingly after choosing each PRI. For PRIs four onwards, decodability must be checked between each PRI in the set \mathcal{P} and each combination of pair of the PRIs already chosen. This process will ensure that the PRI set is fully decodable. If $|\mathcal{P}| = 0$ before all the PRIs are chosen, the objective is set to be totally blind.

The objective function provides a measure of how well an individual performs in the problem domain [7]. In this case, the objective function is the total area of the blind zone map

TABLE II

PERFORMANCE OF EVOLUTIONARY ALGORITHM OVER 100 TRIALS FOR 3 OF 8 DECODING.

Best	58.37%
Worst	59.91%
Mean	59.01%
Median	59.02%
σ	0.28%

(in metres Hertz) with four or more PRFs clear. The decoding process has already ensured that the PRF set is fully decodable with reduced ghosting and no has blind velocities.

A simple evolutionary programme [8] with a base population of $M = 50$ trial solutions was used as the evolutionary engine. The evolutionary programme operates by creating $N = 50$ new trial solutions at each generation, and evaluating them for blind zone performance. The best 50 overall from the $N + M$ set are then chosen for the next generation. In this particular algorithm, an initial population of 100 trial solutions was used, of which the best 50 were chosen for generation 1. Evolutionary programmes are very simple, yet very powerful optimisation algorithms.

To create the 50 new solutions a typical evolutionary programme cycle of crossover and mutation was applied. First the 50 chromosomes remaining in the previous generation were copied. Each of the 50 solutions had a 70% chance of being crossed during the copy with another chromosome chosen at random from the population (with replacement). The 70% probability of crossover was chosen as it provided reasonably consistent convergence performance, although the value of the parameter is not critical and values in the range 50% to 90% are unlikely to provide a significant difference in performance. If crossover was to be performed, real valued intermediate crossover [7], as detailed in equation 1, was used to recombine the genes, where G_{a_i} and G_{b_i} are gene i of the new chromosome a and the chromosome b , with which to cross. The value r_i is a uniform random number in the range $[0,1]$, selected anew for each gene. Intermediate crossover is a standard technique and will produce new solutions that are similar to both the parent chromosomes. For example, if the chromosomes

$$a = [0.5 \quad 0.3 \quad 0.2 \quad 0.8 \quad 0.7 \quad 0.6 \quad 0.9 \quad 0.1]$$

and

$$b = [0.2 \quad 0.7 \quad 0.3 \quad 0.8 \quad 0.9 \quad 0.4 \quad 0.2 \quad 0.5]$$

were to be combined with crossover, first a random number corresponding to each gene location must be generated and then (1) applied. If the set of random numbers was

$$r = [0.3 \quad 0.6 \quad 0.3 \quad 0.2 \quad 0.6 \quad 0.3 \quad 0.5 \quad 0.2]$$

then the resulting child chromosome would be

$$c = [0.44 \quad 0.56 \quad 0.22 \quad 0.80 \quad 0.83 \quad 0.56 \quad 0.55 \quad 0.12]$$

$$G_{c_i} = G_{a_i} + (1.5r_i - 0.25)(G_{b_i} - G_{a_i}) \quad i = 1 \dots n \quad (1)$$

Gaussian mutation was then applied to each gene by adding a random number drawn from a zero-mean Gaussian distribution with an initial standard deviation of 0.125. The initial standard deviation is chosen as 1/8 of the range of the gene values. A new random number is drawn for each gene in each chromosome. The algorithm was forced to converge by reducing the standard deviation of the Gaussian distribution used for the mutation process by multiplying by a factor of 0.9 every generation. Thus as the algorithm progresses, the size of the random numbers added to the genes reduces and forces the search to be refined in order to provide more repeatable results in a limited number of generations. In the first few generations of the evolutionary algorithm, the mutations are large and so a wide search is performed

across the PRI search space. The reduction factor of 0.9 reduces the standard deviation of the mutations quite quickly, so after around 30 generations, the mutation, and therefore the global search, is having little effect. The search direction is controlled more by crossover and therefore local exploitation of the optimisation surface is performed.

The algorithm was terminated after 100 generations and the best solution selected (i.e. best blind zone performance) as the final PRI set for use. This size of population and number of generations provided a reasonable number of sample solutions from the problem domain without incurring unmanageable processing times.

D. Summary

The maximum transmitter duty cycle (20%) constrains the maximum acceptable PRF to be 28.57kHz. The width of the mainbeam clutter rejection notch (± 1.67 kHz) constrains the minimum PRF to be 6.67kHz, allowing the clutter to occupy up to a maximum of half the PRF. The PRI constraints, combined with the chromosome transformation algorithm means all PRI sets are decodable, retain good target visibility and are not prone to blind velocities. Repeated generations of the evolutionary algorithm optimisation process continue to refine target visibility by minimising blind zones, subject to blind velocity and ghosting checks.

V. RESULTS

A. Introduction

Trials of the radar model and evolutionary algorithm were conducted with each experiment having a population of 50 PRI schedules over 100 generations, for a $5m^2$ target. The effectiveness of the evolutionary algorithm routine was initially assessed searching for optimum 8-PRF schedules. Once the ability of the evolutionary algorithm to find optimum, or near-optimum, 8-PRF schedules was confirmed, the evolutionary algorithm was tasked with searching for optimum 9-PRF schedules.

B. Optimum 8-PRF Schedules

Each of the experiments was repeated 100 times in order to generate statistics on the repeatability of the evolutionary algorithm results. Table II shows the statistics for the 3 of 8 problem, with the performance indicated by the percentage of the blind zone map that has fewer than four PRFs clear.

Figure 7 shows the blind zone map for the best 3 of 8 solution found. Table III shows the PRIs used, the mean PRI, mean duty cycle and range-Doppler area that is blind. For an 8 PRF schedule, the mean PRI must be less than $100.4\mu s$ (assuming 65ms

TABLE III
PRI SET FOR BEST 3 OF 8 STRATEGY (μs)

63.11	69.97	77.07	81.31	90.06	99.90	109.75	119.00
Mean PRI						88.77 μs	
Mean duty cycle						7.89 %	
Peak duty cycle						11.09 %	
Min range/Doppler blindness (m.Hz)						1.0629e+10	

TABLE V
PRI SET FOR BEST 3 OF 9 STRATEGY (μs)

65.00	65.62	72.41	79.96	83.92	88.44	93.30	102.84	112.41
Mean PRI						84.88 μs		
Mean duty cycle						8.25 %		
Peak duty cycle						10.77 %		
Min range/Doppler blindness (m.Hz)						9.7876e+9		

TABLE IV
PERFORMANCE OF EVOLUTIONARY ALGORITHM OVER 100 TRIALS FOR 3 OF 9 DECODING.

Best	53.74%
Worst	55.02%
Mean	54.46%
Median	54.51%
σ	0.26%

dwel time and 1.7ms lost per PRI in change over). The mean PRI identified could either be used with a scan rate of $66.0^\circ/\text{s}$, or dead time / built-in-test could be added at the end of the set of PRIs, as is used in many current radar systems. Often the scan rate is determined by subsequent processing but with phased array technology becoming more available in airborne systems, the pressure to allow a variable scan rate is increasing.

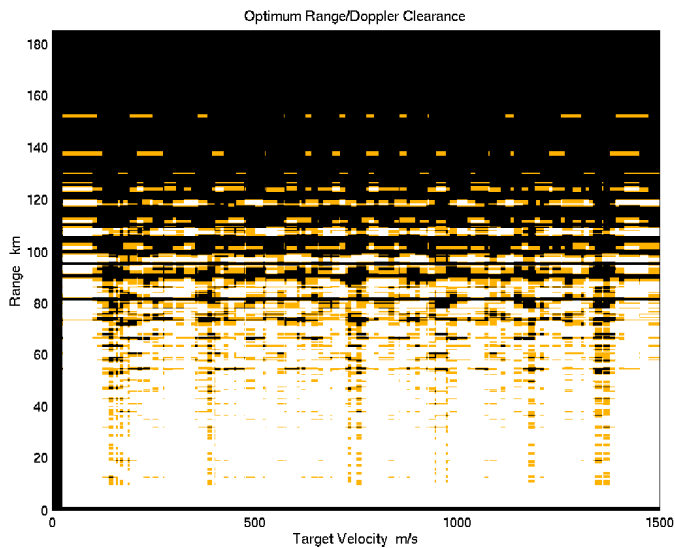


Fig. 7. Blind zone map for best 3 of 8 solution, 5 m^2 target

C. Optimum 9-PRF Schedules

Table IV shows the statistics for the 3 of 9 problem, with the performance indicated by the percentage of the blind zone map that has fewer than four PRFs clear.

Figure 8 shows the blind zone map for the best 3 of 9 solution found. Table V shows the PRIs used, the mean PRI, mean duty cycle and range-Doppler area that is blind. For a 9 PRF schedule, the mean PRI must be less than $86.3 \mu\text{s}$. The mean PRI identified corresponds to a scan rate of $60.8^\circ/\text{s}$.

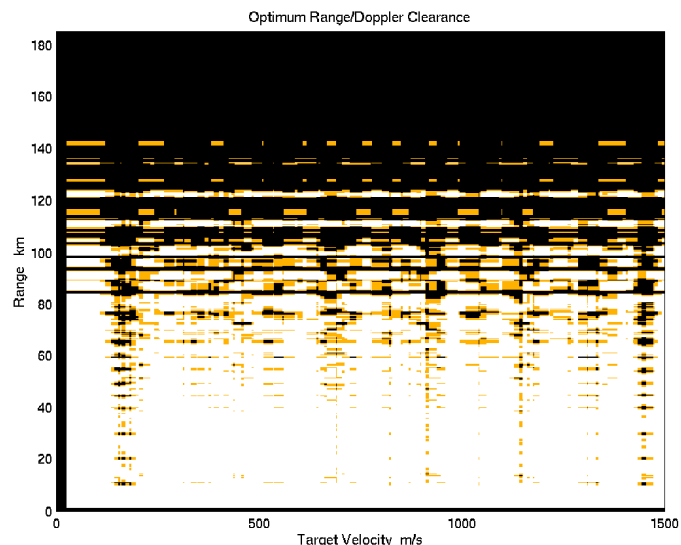


Fig. 8. Blind zone map for best 3 of 9 solution, 5 m^2 target

D. Evolutionary algorithm Performance

With each run of the search routine, different near-optimum PRF schedules are found, although the range-Doppler blindness varies marginally (by about 1-2%). This implies that the PRI search space contains many local optimum solutions with similar range-Doppler blindness performances. The average and peak duty cycles of these solutions are found to be consistent with those of some modern fielded radars.

With the optimisation being performed against small targets with respect to the clutter, large black areas occur towards the top of the blind-zone map due to the sidelobe clutter levels. With larger targets, the long-range region of the blind zone map is clearer, as demonstrated in figure 9 which is calculated for a 10 m^2 target. Figures 7, 8 & 9 all show blind zone maps that are fully decodable and have no blind ranges.

With code that has not been optimised for speed and on a modern desktop computer (1GHz Pentium 3), each run of the evolutionary algorithm takes approximately 3 hours. This is reduced to approximately 70 minutes on a DEC Alpha 667MHz EV67 processor. By optimising the code for speed and with faster processing becoming available each year, the processing times are expected to be reduced significantly in the near future.

E. Number of PRFs in the Schedule

Typically, 8-PRF schedules are employed in fielded radar systems. Eight PRFs are traditionally thought to be a reasonable compromise between the requirement to overcome range-Doppler blindness and the ability to transmit the entire PRF

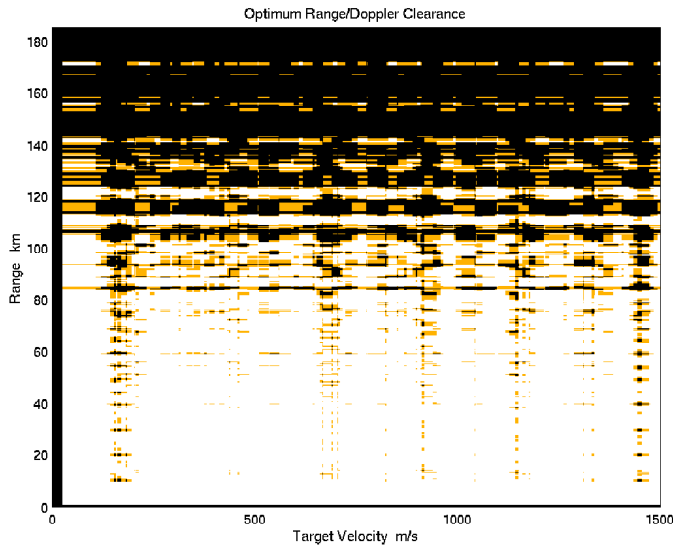


Fig. 9. Best 3 of 9 schedule but with $10m^2$ target

schedule within the dwell time on target. Moreover, searching for longer PRF schedules using conventional search techniques becomes increasingly more difficult. However, this study has demonstrated the efficiency and power of evolutionary algorithm techniques when applied to this type of combinatorial problem. Not only is the evolutionary algorithm able to find optimum or near optimum 8-PRF schedules within reasonable time frames but the evolutionary algorithm is able to find optimum or near-optimum 9-PRF schedules with similar efficiency.

VI. CONCLUSIONS

The use of the Chinese Remainder Theorem for decoding returns from each burst constrains the choice of PRF to such an extent that PRF sets must be selected solely for decodability. Optimisation of PRF sets for other issues is not practical.

The use of the coincidence algorithm permits PRIs to be selected with the resolution of the clock period ($=10ns$ in our example). This improved resolution increases the number of PRIs but enables selection to be optimised for decodability, blindness, blind velocities and ghosting.

The evolutionary algorithm can select near-optimal PRF sets efficiently, with modest computing effort and produce a significant improvement in radar detection performance. The ‘quality’ of each set is based on models of airborne fire control radar and associated clutter and so each PRF set is application/scenario specific.

Repeated runs of the evolutionary algorithm identify near-optimal PRF sets which differ marginally from each other. These repeats indicate the existence of several similar local optima in the problem space and the ability of the evolutionary algorithm to find them.

The evolutionary algorithm has optimised the selection of 3 of 9 schedules which may be transmitted within the target illumination time. Although 9-PRF schedules are more difficult to transmit within the dwell time, the advantage gained is a marked improvement in range-Doppler blindness. Typically, with a $5m^2$ RCS target and the particular clutter characteristics applied in

the model, a 4.6% improvement in total range-Doppler blindness is achieved over an 8-PRF system, with the most noticeable improvement occurring at the medium detection ranges (60 to 120 Km), beyond which high sidelobe clutter levels are the dominant cause of blindness. Of all the near-optimum PRF schedules found, the 9-PRF schedule detailed in Table V has the best blind zone performance against the standard $5m^2$ target.

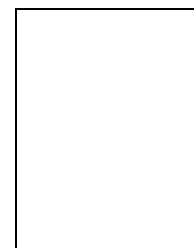
The evolutionary algorithm could be developed to run much quicker; even to the extent of optimising the selection dynamically to run in real time.

ACKNOWLEDGEMENTS

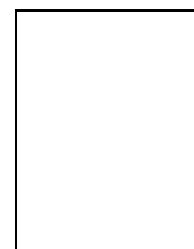
The authors would like to acknowledge the use of the Department of Aerospace, Power, and Sensors DEC Alpha Beowulf cluster for this research.

REFERENCES

- [1] P. G. Davies and E. J. Hughes, “Medium PRF set selection using evolutionary algorithms,” *IEEE Transactions on Aerospace and Electronic Systems*, 2002, to Appear.
- [2] William H. Long and Keith A. Harringer, “Medium PRF for the AN/APG-66 radar,” *Proceedings of the IEEE*, vol. 73, no. 2, pp. 301–311, Feb. 1985.
- [3] J. Simpson, “PRF set selection for pulse Doppler radars,” in *IEEE Region 5 Conference, 1988: ‘Spanning the Peaks of Electrotechnology’*, 1988, pp. 38–44.
- [4] R. A. Moorman and J. J. Westerkamp, “Maximizing noise-limited detection performance in medium PRF radars by optimizing PRF visibility,” in *Proceedings of the IEEE 1993 National Aerospace and Electronics Conference, NAECON 93*, 1993, vol. 1, pp. 288 – 293.
- [5] Merrill I. Skolnik, Ed., *Radar Handbook*, McGraw-Hill, 2nd edition, 1990, ISBN 0-07-057913-X.
- [6] Guy V. Morris, *Airborne Pulsed Doppler Radar*, Artech House, Norwood, MA, 1988, ISBN 0-89006-272-2.
- [7] A. M. S. Zalzal and P. J. Flemming, Eds., *Genetic algorithms in engineering systems*, The Institution of Electrical Engineers, 1997.
- [8] David E. Goldberg, *Genetic Algorithms in Search, Optimization, and Machine Learning*, Addison-Wesley Publishing Company, Inc., 1989.

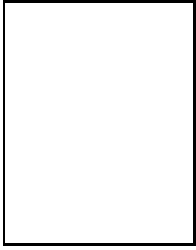


Clive M. Alabaster received his BSc degree in Physics with Microelectronics from University College Swansea, Wales, in 1985. From 1985 to 1992 he worked as a microwave design and development engineer (on airborne radar systems) with GEC Marconi, Milton Keynes. From 1992 to 1998 he worked as a lecturer in radar techniques at Arborfield Garrison, near Reading. He joined Cranfield University at the Royal Military College of Science, Shrivenham, in 1998 as a lecturer in the Radar Systems group within the Department of Aerospace, Power and Sensors. He is also registered for a Ph.D. and is researching the electrical properties of lossy dielectrics. He is a member of the Institute of Physics and is a Chartered Engineer. Email: C.M.Alabaster@rmcs.cranfield.ac.uk



Dr. Evan J. Hughes Received his BEng and MEng degrees in Electrical and Electronic Engineering from the University of Bradford, England, in 1993 and 1994 respectively. From 1993 to 1995 he worked as a design engineer with GEC Marconi, Leicester. He received his Ph.D. in 1998 from Cranfield University at the Royal Military College of Science, Shrivenham, England. His primary research interests include noisy multi-objective evolutionary algorithms, swarm guidance, data fusion, artificial neural networks, fuzzy systems, intelligent agents and radar systems. He is a member of both the IEE and the IEEE and is a Chartered Engineer. He received the prize for best paper at GALEZIA '97, Glasgow, UK, won the Evolutionary

Checkers Competitions at CEC 2001, Seoul, S. Korea and WCCI 2002, Honolulu, Hawaii, and won the Time Series Prediction Competition at WCCI 2002. He is currently working as a lecturer for the Radar Systems group in the Department of Aerospace, Power and Sensors. Email: ejhughes@iee.org



John H. Matthew Received his BSc degree in Engineering from the University of Durham, England, in 1992. From 1992 to the present he has served in the Royal Air Force as a Communications Electronics Engineering Officer, working primarily in the field of military airfield navigation aids. He received his MSc degree in Military Electronic Systems Engineering from Cranfield University at the Royal Military College of Science, Shrivenham, England, in 2001. Since then he has been working in the field of airborne intercept radars. He is an associate member of

the IEE.